The Chloroazaphosphatrane Motif for Halogen Bonding in Solution

Chunyang Li, Anne-Doriane Manick, Jian Yang, David Givaudan, Bohdan Biletskyi, Sabine Michaud-Chevalier, Jean-Pierre Dutasta, Damien Hérault, Xavier Bugaut, Bastien Chatelet, et al.

The Chloroazaphosphatrane Motif for Halogen Bonding in Solution

Chunyang Li,[§] Anne-Doriane Manick,[§] Jian Yang, David Givaudan, Bohdan Biletskyi, Sabine Michaud-Chevalier, Jean-Pierre Dutasta, Damien Hérault, Xavier Bugaut,* Bastien Chatelet,* and Alexandre Martinez*

ABSTRACT: Chloroazaphosphatranes, the corresponding halogenophosphonium cations of the Verkade superbases, were evaluated as a new motif for halogen bonding (XB). Their modulable synthesis allowed for synthetizing chloroazaphosphatranes with various substituents on the nitrogen atoms. The binding constants determined from NMR titration experiments for Cl^-, Br^-, I^-, AcO^-, and CN^- anions are comparable to those obtained with conventional iodine-based monodentate XB receptors. Remarkably, the protonated azaphosphatrane counterparts display no affinity for anions under the same conditions. The strength of the XB interaction is, to some extent, related to the basicity of the corresponding Verkade superbase. The halogen bonding abilities of this new class of halogen donor motif were also revealed by the $\Delta\delta(^{31}P)$ NMR shift observed in CD_2Cl_2 solution in the presence of triethylphosphine oxide (TEPO). Thus, chloroazaphosphatranes constitute a new class of halogen bond donors, expanding the repertory of XB motifs mainly based on C_{Ar}–I bonds.

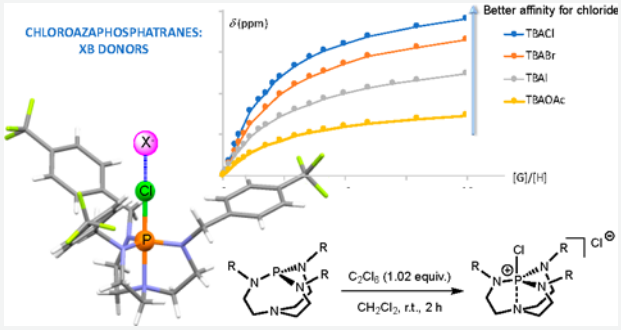

INTRODUCTION

Anion recognition plays a crucial role in medicine, biology, chemistry, and environmental sciences.[1,2] Synthetic anion receptors have thus found various applications, ranging from sensors, organocatalysts, or anion carriers in living systems to the remediation of toxic or radioactive anions from aqueous wastes.[3−15] As a consequence, the development of new motifs for anion binding arouses a considerable interest. Behind the traditional interactions often used to recognize anions, such as hydrogen bonding, dispersion forces, or electrostatic interactions, less common interactions, like anion−π interactions,[16−18] coordination with Lewis acid (metals or main group elements),[19−21] or σ−hole interactions[22−27] have recently received growing attention, leading to the expansion of anion receptors and to the improvement of the selectivity and binding strength.

Among the σ−hole interactions, XB (halogen bonding) interaction appears as the most studied for anion recognition.[28] Indeed, its strength and strong directionality have led to its wide use in materials design and crystal engineering[29−31] and have found more recent applications in the solution phase for anion recognition, transport and sensing, or organocatalysis.[32−41] Although the XB-anion receptors display a large range of various structures, from acyclic compounds to interlocked molecules,[42−47] the XB motifs used are still mainly limited to neutral or cationic hetero- or carbocycles (e.g., haloperfluoroarene, halotriazole, halotriazolium, haloimidazolium, and halopyridinium motifs). These XB donors are based on halogen atoms bounded to carbon atoms included in an aromatic cycle, inhibiting a possible nucleophilic substitution that could occur on aliphatic ones, in the presence of anions. Several requirements need to be fulfilled to build new XB donors: (i) the system must include a halogen atom linked to an electrodeficient unit, (ii) it must be stable in the presence of nucleophilic anions or other Lewis bases, and (iii) ideally their synthesis should be easy and highly modulable.

In this context, haloazaphosphatranes appear as a promising motif for XB (Chart 1).[48] Indeed, their non-halogenated derivatives, the proazaphosphatranes, also named Verkade's superbases,[49,50] are highly basic non-ionic organic compounds that have found a considerable range of applications, for instance, as catalysts or stoichiometric reagents.[51−59] This strong basicity is related to the remarkable stability of their acidic counterparts, the azaphosphatranes. This stability is due to the formation, upon protonation, of a transannular bond between the apical nitrogen and the phosphorus atom, leading to the formation of three five-membered rings and the delocalization of the positive charge on the four nitrogen

Chart 1. General Structure of Proazaphosphatrane (1), Azaphosphatrane (1-H$^+$), and Haloazaphosphatrane (1-X$^+$, with X = F, Cl, Br, or I)[a]

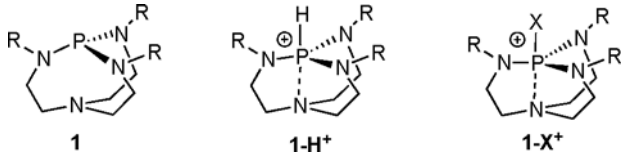

[a]Counterions are omitted for clarity.

atoms.[60] Compared to proazaphosphatranes, the azaphosphatranes have only recently attracted attention and were shown to act as hydrogen bond donors for (i) anion complexation in water when included in self-assembled cages[61,62] or (ii) organocatalysis in ROP reaction,[63] CO_2 conversion,[64] and Strecker reaction.[65] Even though the synthesis and characterization of their halogenated parents have been reported,[66−68] this class of compounds has never found applications. We hypothesized that the strong stability of the azaphosphatranes might be retained to some extent in the haloazaphosphatranes and that the electron-withdrawing effect of the positive phosphorus atom should allow XB formation. Moreover, the substituents on the nitrogen atom can be easily varied, allowing a modulation of the stereoelectronic properties of the haloazaphosphatranes.

Herein, we report on the synthesis and anion binding properties of the five chloroazaphosphatranes **(1a−1e)-Cl$^+$·PF$_6^-$** bearing various substituents on the nitrogen atoms (Scheme 1). NMR titrations led to the determination of the binding constants in the range of 50 M^{-1}, comparable with other "classical" monodentate motifs such as iodoperfluorobenzene or iodoimidazolium.[69,70]

RESULTS AND DISCUSSION

Synthesis of Chloroazaphosphatranes. Taking advantage of the versatility of their synthesis, the four known azaphosphatranes **(1a−1d)-H$^+$** and the new one **1e-H$^+$**, were synthesized in two steps (Scheme 1): the reductive amination between the tris(2-aminoethyl)amine (tren) unit **2** and chosen aldehydes followed by a reaction with $PCl(NMe_2)_2$ provided the azaphosphatranes bearing various substituents on the nitrogen atoms.[71,72] Then, the corresponding proazaphosphatranes **1a−1e** were obtained by deprotonation of the azaphosphatranes by *t*BuOK in CH_2Cl_2. The two previously reported chloroazaphosphatranes **1a-Cl$^+$·Cl$^-$** and **1b-Cl$^+$·Cl$^-$** and the three new ones **1c-Cl$^+$·Cl$^-$**, **1d-Cl$^+$·Cl$^-$**, and **1e-Cl$^+$·Cl$^-$** were obtained in good yields after reaction of the corresponding proazaphosphatranes with hexachloroethane for 2 h at room temperature.[66−68] However, the subsequent anion exchanges were revealed to be unsuccessful in the presence of water, but the use of acetonitrile as solvent allowed for the anion metathesis of the chloride anion by the PF_6^- one. For **1d-Cl$^+$·Cl$^-$**, anion metathesis of the chloride anion with BAr^{F-} was also performed. Because of the potential interest of the bromo and iodo analogues, attempts to isolate the **1-Br$^+$·PF$_6^-$** or **1-I$^+$·PF$_6^-$** compounds using the same sequence of reactions were performed. However, they were unsuccessful in our hand, probably because of the higher sensitivity of these compounds even to weak nucleophiles such as water or alcohols. Thus, the desired compounds **(1a−1e)-Cl$^+$·PF$_6^-$** and **1d-Cl$^+$.BAr^{F-}** were obtained in five steps from the commercial tris(2-aminoethyl)-amine compound and the corresponding aldehydes in 20−38% yields.

Characterization of Chloroazaphosphatranes. The chloroazaphosphatranes were characterized by means of ^1H, ^{13}C, and ^{31}P NMR spectroscopy and mass spectrometry (see the Supporting Information). The ^{31}P NMR chemical shifts of **1a-Cl$^+$**, **1c-Cl$^+$**, **1d-Cl$^+$**, and **1e-Cl$^+$** are between −22.5 and −19.04 ppm (Figures S51, S59, S63, and S67, respectively), values that are similar to those previously reported for **1a-Cl$^+$**.[68] In contrast, **1b-Cl$^+$** exhibits a signal at −4.32 ppm (Figure S55), suggesting some specific structural features (vide infra).[67]

Crystals of **1a-Cl$^+$·PF$_6^-$** and **1e-Cl$^+$·PF$_6^-$** suitable for X-ray diffraction analysis were obtained by crystallization in a mixture of Et_2O/CH_3CN, and the resulting structures (Figure 1) were compared with those reported for **1a-Cl$^+$·ClBPh$_3^-$** and

Scheme 1. Synthesis of Chloroazaphosphatranes 1-Cl$^+$·PF$_6^-$

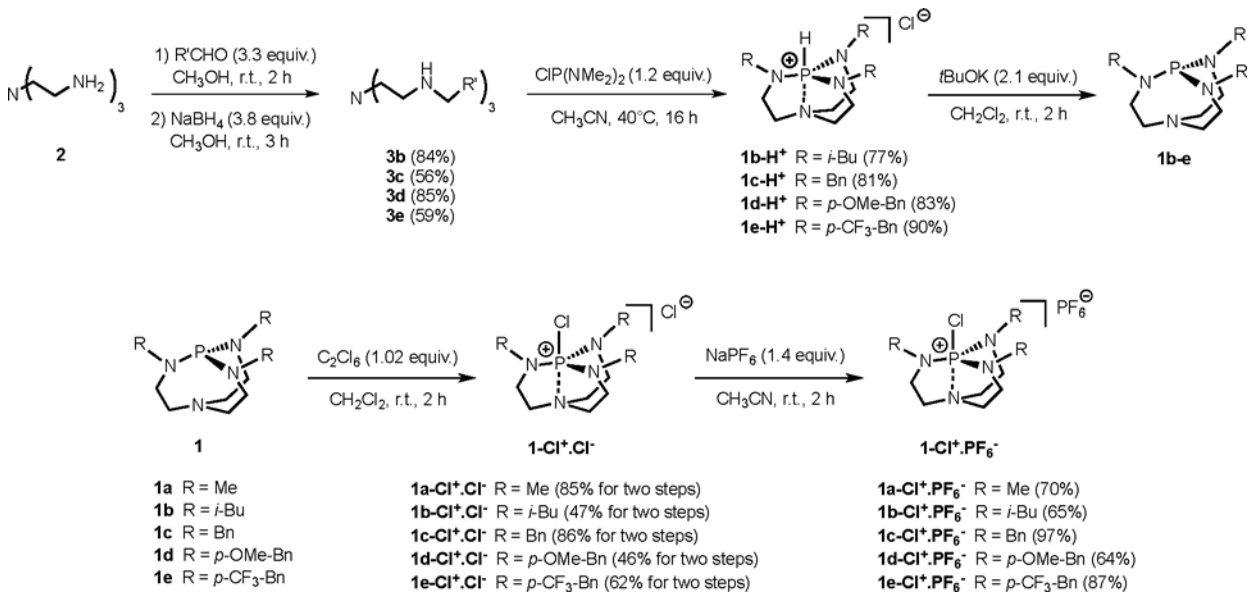

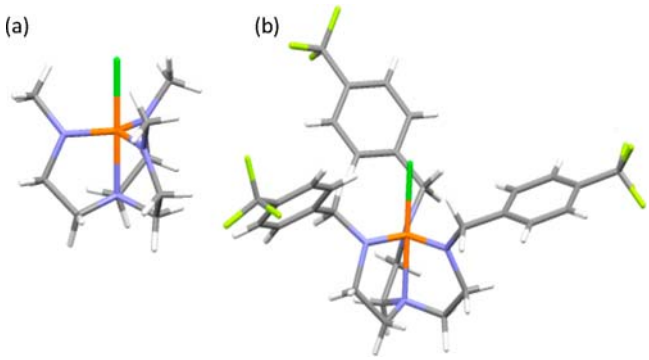

Figure 1. X-ray molecular structures of **1a-Cl**$^+$ (a) and **1e-Cl**$^+$ (b) cations.

1b-Cl$^+$**·PF$_6$**$^-$ (Table 1).[67,68] The structures of **1a-Cl**$^+$**·PF$_6$**$^-$ and **1a-Cl**$^+$**·ClBPh$_3$**$^-$ salts are almost similar, showing that these noncoordinating anions have little influence on the structure of the chloroazaphosphatrane cations in the solid state. In the four structures, the phosphorus atom adopts a pseudo-trigonal bipyramidal geometry and the apical nitrogen presents a pseudo-pyramidal one. Whereas the P−Cl bond lengths are similar in all three of these structures (2.1 Å), the P−N$_{axial}$ distances differ more strongly with 1.939 and 1.960 Å in **1a-Cl**$^+$**·PF$_6$**$^-$ and **1e-Cl**$^+$**·PF$_6$**$^-$, respectively, and 2.128 Å in **1b-Cl**$^+$**·PF$_6$**$^-$. Moreover, the azatrane structures adopt a helical arrangement in **1a-Cl**$^+$**·PF$_6$**$^-$ and **1e-Cl**$^+$**·PF$_6$**$^-$, while the C$_5$-membered rings in the azaphosphatrane **1b-Cl**$^+$**·PF$_6$**$^-$ present eclipsed conformations (see dihedral angle C−N$_{ax}$−P−N$_{eq}$ in Table 1 and Figures S2 and S4). The steric hindrance of the isobutyl groups might account for the more elongated transannular distance and the specific conformation of the atrane structure in **1b-Cl**$^+$**·PF$_6$**$^-$. These structural features are also probably retained in solution, which could account for the peculiar ^{31}P NMR chemical shift observed for **1b-Cl**$^+$**·PF$_6$**$^-$.

Anion Binding Properties. The anion binding properties of the chloroazaphosphatranes were studied by ^{1}H NMR titration experiments at 298 K, using acetonitrile as solvent. The chloroazaphosphatranes were stable under the conditions used during the titration experiments, and no decomposition was observed. Figure 2a shows the typical changes observed in the ^{1}H NMR spectrum of **1a-Cl**$^+$**·PF$_6$**$^-$ upon progressive addition of tetrabutylammonium (TBA) chloride salt. Compounds **(1a−1e)-Cl**$^+$**·PF$_6$**$^-$ display only one set of signals during the titration experiments, showing that the XB process is in fast exchange on the NMR time scale (Figures S89−S103). For all chloroazaphosphatranes, the signals of the protons of the bridging methylenes clearly exhibit downfield shifts, whereas those of the R groups grafted on the equatorial nitrogen atoms displayed smaller NMR shifts. This suggests that these substituents are not directly involved in the recognition process but more probably only affect the electronic properties of the chloroazaphosphatranes. Thus, the interaction between anion and σ-hole might impact the transannular bond length, inducing changes in the chemical shifts of the methylene protons. The interaction between the **1d-Cl**$^+$**·PF$_6$**$^-$ receptor and the iodide anion was also monitored by ^{31}P NMR. A change in the chemical shift of around 0.3 ppm was observed (Figure S99). This is consistent with a close proximity of the phosphorus atom to the binding site. Furthermore, this experiment also supports that no direct reaction between the nucleophilic anion and the electrophilic phosphorus atom occurs, since such a reaction should lead to higher changes in the chemical shift; indeed, the difference in ^{31}P NMR between a chloro- and a iodo-azaphosphatrane is more than 20 ppm. This lack of reactivity at the phosphorus is in agreement with the unique stability of the azaphosphatrane structure described by J. G. Verkade.[48,51] Furthermore, to highlight the crucial role of the Lewis basicity of the anion and the negligible role played by the TBA cation, a titration experiment has been carried out with the TBA$^+$PF$_6$$^-$ salt (Figure S98). No change in the ^{1}H chemical shifts of the chloroazaphosphatrane **1d-Cl**$^+$**·PF$_6$**$^-$ was observed during this experiment, evidencing the crucial role of halogen bonding in the recognition of anions by this class of receptor.

The titration curves were obtained by plotting the complexation-induced shifts of the methylene protons as a function of the halide/receptor ratio. In all cases, the corresponding resonances are well-defined and sharp and display no overlapping with other signals. Modeling of these curves with the Bindfit program allowed for the determination of the binding constants, the 1:1 anion:receptor association providing the best fit, to give the binding constants K_a reported in Table 2.[73,74] First of all, we note that the binding constant values are modest, from 20 to 50 M^{-1}, but importantly, they are in the same order of magnitude as those obtained with other "classical" monodentate XB receptors like iodoperfluorobenzene (C_6F_5I) or iodoimidazolium.[69,70]

This is all the more remarkable that these last two motifs benefit from the high polarizability of the iodine atom to create an important electrophilic σ-hole, whereas the low polarizability of the chlorine atom in the chloroazaphosphatranes is less suitable to induce halogen bonding. Here, although the chlorine atom is used as a XB donor, association constants comparable with iodine-based monodentate receptors are reached, showing the great potentiality of this motif to build multidentate XB donors or to be combined with other interactions to design even more efficient receptors. Moreover, when BAr^{F-} was used as a counterion instead of PF$_6$$^-$, no significant change in the value of the binding constant was observed: K_a values of 43 and 45 M^{-1} were obtained for **1d-Cl**$^+$**·PF$_6$**$^-$ and **1d-Cl**$^+$**.BAr^{F-}**, respectively, with chloride as the guest anion (Table 2, entry 4).

A second feature concerns the affinities of the five chloroazaphosphatranes for the chloride anion, which are

Table 1. Selected Crystallographic Parameters for 1a-Cl$^+$·PF$_6$$^-$, 1b-Cl$^+$, and 1e-Cl$^+$ Cations

	d_{PCl} (Å)	d_{PNax} (Å)	d_{PNeq} (Å)	$\Sigma_{Neq-P-Neq}$ (deg)	$\Sigma_{C-Nax-C}$ (deg)	dihedral angle C−N$_{ax}$−P−N$_{eq}$ (deg)
1a-Cl$^+$ [a]	2.101	1.928	1.663	359.1	336.0	29.4
1a-Cl$^+$ [70] [b]	2.123	1.939(2)	1.656	358.8(8)	339.3	35.6
1b-Cl$^+$ [69]	2.109	2.128(7)	1.643	354.2(7)	340.9(9)	1.1(8)
1e-Cl$^+$	2.112(3)	1.960(2)	1.662(2)	358.3(3)	339.6(6)	32.8(2)

[a] PF$_6$$^-$ as counterion. [b] ClBPh$_3$$^-$ as counterion.

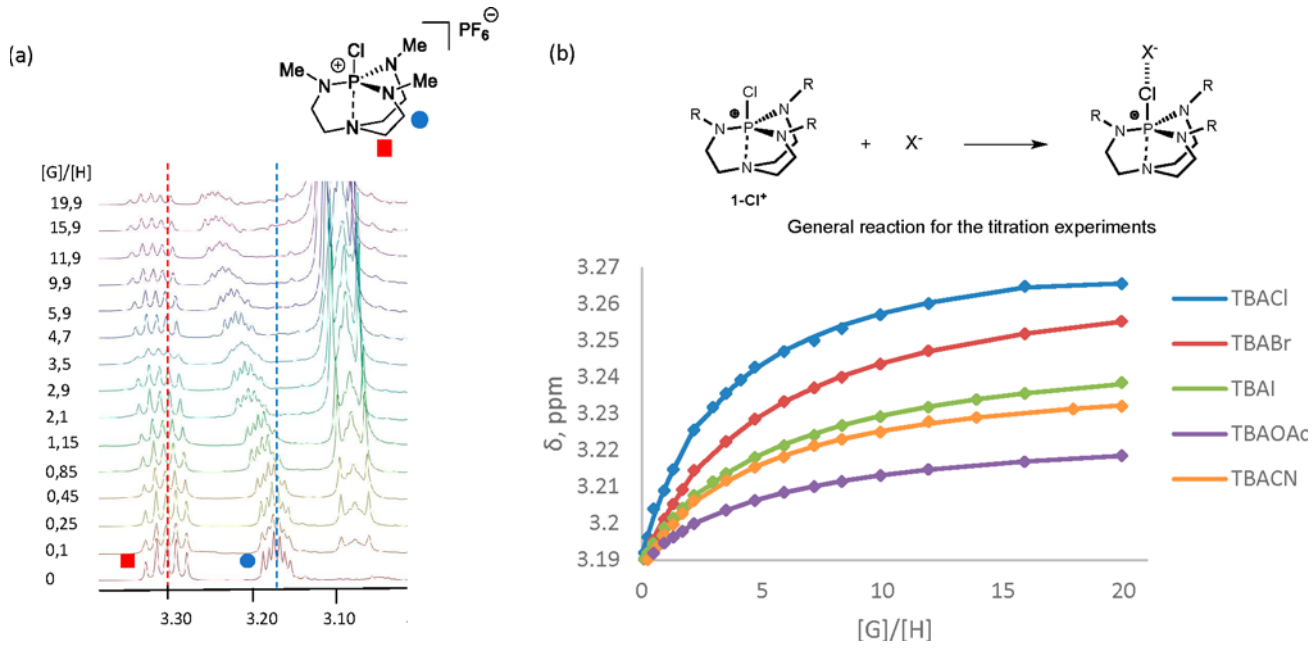

Figure 2. (a) Example of the ^{1}H NMR monitoring of the titration of host **1a-Cl$^+$·PF$_6^-$** (5 mM) with Cl$^-$ (as a 50 mM solution of TBACl salt) in CD_3CN; (b) titration curves of host **1a-Cl$^+$·PF$_6^-$** with TBA-halide and acetate salts in CD_3CN. The chemical induced shifts $\Delta\delta$ of the host's protons at 3.18 ppm were measured and plotted as a function of the [G]/[H] ratio. Curves fitted with the Bindfit program (lines). Blue, Cl$^-$; red, Br$^-$; green, I$^-$; purple, AcO$^-$; orange, CN$^-$.

Table 2. Binding Constants K_a (M^{-1}) for the 1:1 Complexes Formed between (1a−1e)-Cl$^+$ and Anion Guests in CD_3CN[a]

entry	receptor	Cl$^-$	Br$^-$	I$^-$	AcO$^-$	CN$^-$	pK_a
1	**1a-Cl$^+$·PF$_6^-$**	32	26	18	22.5	27	32.90[60]
2	**1b-Cl$^+$·PF$_6^-$**	22	21	29	24	*d*	33.53[60]
3	**1c-Cl$^+$·PF$_6^-$**	51	26	20	20	42	31.80[c]
4	**1d-Cl$^+$·PF$_6^-$**	43[b]	31	26	23	35	32.14[58]
5	**1e-Cl$^+$·PF$_6^-$**	55	39	33	26	39	29.80[c]

[a] K_a were determined by fitting ^{1}H NMR titration curves (CD_3CN, 500 MHz, 298 K) of the methylene protons of the chloroazaphosphatranes (see the Supporting Information) with the Bindfit program. More details on the calculation results (covariance and RMS) can be found in Table S1; estimated error 10%. [b] K_a = 45 M^{-1} when BAr^{F-} was used as the counterion instead of PF$_6^-$. [c] See the Supporting Information for the determination of the pK_a of these two proazaphosphatranes. [d] The formation of a precipitate was observed during the titration experiment.

higher than those for the bromide and iodide, as expected from the stronger basicity of the former. For instance, binding constants of 55, 39, and 33 M^{-1} were respectively obtained for Cl$^-$, Br$^-$, and I$^-$ anions when **1e-Cl$^+$·PF$_6^-$** was used as the halogen bond donor (entry 5, Table 2). We then examined if the binding constant could be related to the basicity of the corresponding Verkade superbase. The pK_a values of **1a**, **1b**, and **1d** are known from the literature, and those of **1c** and **1e** were estimated from competition experiments using our previously described procedure (Table 2; Figures S87 and S88).[58] It appears that the affinity of the chloroazaphosphatranes for the chloride anion decreases with the basicity of the proazaphosphatrane parents. This is consistent with the ability of the substituents to stabilize the positive charge on the phosphorus atom: the most basic proazaphosphatrane corresponds to the most stable azaphosphatrane, and thus probably to a less electrophilic σ-hole in the corresponding chloroazaphosphatrane. For other anions, the binding constants are too close to allow for relevant comparisons. Nevertheless, the receptor **1e-Cl$^+$·PF$_6^-$**, associated with the less basic superbase **1e**, displays the better binding constant whatever the anion used, in agreement with the trend observed for chloride anion. HSO_4^- and $H_2PO_4^-$ were also tested as guests (TBA salts): whereas the former gives a low binding constant of 16 M^{-1} with **1d-Cl$^+$·PF$_6^-$** as a XB donor, a solid precipitate was formed during the titration with the latter one, suggesting the formation of insoluble aggregates between chloroazaphophatranes and dihydrogenophosphate anions.

Comparison of Chloroazaphosphatranes with Azaphosphatranes and Fluoroazaphosphatranes. Characterizing the real nature of non-covalent interactions is a thorny question, especially for XB donors. Titration experiments were also carried out using the **1d-H$^+$·PF$_6^-$** and **1d-F$^+$·PF$_6^-$** salts as receptors in order to examine the role played by the XB interaction in the recognition process. **1d-H$^+$·PF$_6^-$** was obtained by simple anion metathesis in water, whereas **1d-F$^+$·PF$_6^-$** was synthesized using the procedure described by Stephan et al.[68] followed by anion metathesis (see the Supporting Information). When **1d-H$^+$·PF$_6^-$** was used as a receptor, no change in the ^{1}H NMR spectrum was observed upon addition of tetrabutylammonium chloride (TBACl) salt (Figure S104). In particular, the chemical shift of the protons of the methylene bridge and of the P−H unit remain unchanged, showing that no hydrogen bond occurs and supporting that no interaction takes place between the **1d-H$^+$** cation and the chloride anion. During the ^{1}H NMR titration experiment of **1d-F$^+$·PF$_6^-$**, the N−CH$_2$−Ar signal shows no modification and the methylene bridge resonances evidence only extremely small changes, preventing establishing and modeling any titration curve (Figure S106). This is in sharp contrast with the notable changes of the chemical shifts of these protons when **1d-Cl$^+$·PF$_6^-$** is used as a receptor, ruling

Scheme 2. Comparing Chloroazaphosphatranes with Other XB Donors[23]

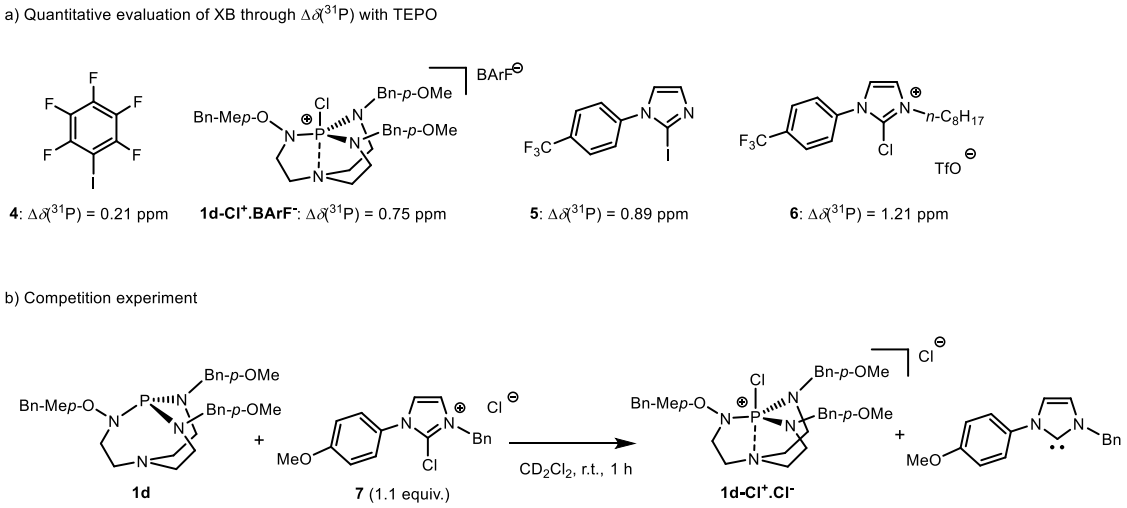

Scheme 3. Chlorazaphosphatrane 1d-Cl$^+$·PF$_6^-$ as the Catalyst for an Aza Diels–Alder Reaction

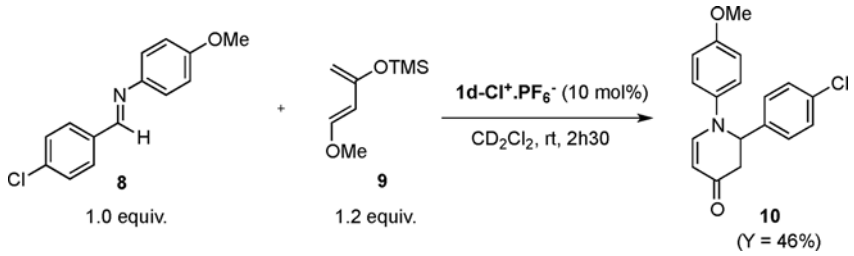

out nondirectional electrostatic interactions, which should have been stronger in the fluorinated analogue, as the main contribution to the observed association. Moreover, this also supports that no direct reaction between the electrophilic phosphorus atom and the nucleophilic anion occurs, as suggested by the ^{31}P NMR study (vide supra). Indeed, such a reaction should be favored when the chlorine is replaced by a fluorine atom: the higher electron-withdrawing properties of the latter probably increases the potential electrophilicity of the phosphorus atom. Thus, neither the **1d-H$^+$·PF$_6^-$** nor the **1d-F$^+$·PF$_6^-$** salts are able to clearly interact with the chloride anion. This indicates that the XB bonding is crucial in this recognition process.

Comparison of Chloroazaphosphatranes with Other XB Donors. As for other Lewis acid–base interactions, comparing the properties of XB donors in solution is a daunting challenge, as the strength of halogen bonding depends on the nature of the Lewis base and the conditions used for titration (method, solvent, concentration).[75,76] Gutmann and Beckett have reported the use of triethylphosphine oxide (TEPO) as a probe to measure the Lewis acidity by ^{31}P NMR spectroscopy.[77,78] Recently, Franz et al. described a unified and easily reproducible procedure to quantify the halogen bonding abilities of different neutral and cationic halogen bond donor motifs, by comparing the ^{31}P NMR shifts of a solution of TEPO in CD_2Cl_2, in the absence and presence of the XB donors.[79] Notably, the downfield shift $\Delta\delta(^{31}P)$ observed when saturating TEPO with an excess of XB donors correlated with their efficiency to catalyze a Friedel–Crafts reaction. With **1d-Cl$^+$·BArF$^-$**, a $\Delta\delta(^{31}P)$ of 0.75 ppm was measured (Scheme 2a and Figure S86); although modest, this value is higher than the one reported for pentafluoroiodobenzene **4** and comparable to those of iodoimidazole **5** and chloroimidazolium **6** (Scheme 2a). This result gives insight into the relative strength of chlorazaphosphatranes compared to other XB donors to induce X-bonding with a Lewis base. To complement this result, a competition experiment was also carried out by mixing proazaphosphatrane **1d** and chloroimidazolium chloride **7** (Scheme 2b). The ^{31}P NMR study of the reaction mixture revealed the transfer of the chlorine atom from the carbon atom of **7** to the phosphorus atom to afford **1d-Cl$^+$·Cl$^-$**, along with the protonation product **1d-H$^+$·Cl$^-$** (Figure S107). This observation is in agreement with the slightly higher XB-donor potency of chloroimidazolium salts compared to chloroazaphosphatranes and the stronger reported basicity of phosphatranes compared to imidazolylidene N-heterocyclic carbenes (NHCs).

Chloroazaphosphatranes as XB Donors in Catalysis. Since the first use of XBs in organocatalysis reported in 2008 by Bolm,[82] XBs revealed various efficient-to-catalyze reactions like Diels–Alder reaction,[83] halogen abstraction,[84] or Michael addition.[85] We therefore decided to evaluate the ability of chloroazaphosphatranes to act as a catalyst using an aza Diels–Alder reaction between the imine **8** and the Danishefsky diene as a benchmark reaction. Imine **8** and diene **9** were mixed in the presence of 0.1 equiv of chloroazaphosphatrane **1d-Cl$^+$·PF$_6^-$** in CD_2Cl_2 at room temperature for 2.5 h (Scheme 3). A yield of 46% was reached, whereas no product was obtained in the absence of chloroazaphosphatrane. From this preliminary result, chloroazaphosphatranes appear as a promising class of XB catalysts.

CONCLUSION

In this work, we have reported the synthesis of five different chloroazaphosphatranes with PF_6^- as a counterion. NMR titration experiments were performed showing that the chloroazaphosphatranes can bind anions with association constants from 20 to 50 M^{-1}, whereas no interaction was detected with both the protonated counterpart azaphosphatranes and the fluoroazaphosphatranes. The substituents on the equatorial nitrogen atoms probably do not interact directly with the anion but modulate the electrophilicity of the σ-hole on the chlorine atom. These results highlight the crucial role of XB in the recognition of anions by chloroazaphosphatranes and make them a new class of relevant motifs for X-bonding with the following features: (i) the XB donor is not a halogen linked to an aromatic carbon, in contrast with most of the classical motifs reported today; (ii) the interaction with anion is comparable to that reached with iodoperfluorobenzene or iodoimidazolium, although a chlorine atom is involved instead of a much more polarizable iodine atom; and (iii) the electronic properties of the R groups on the equatorial nitrogens can tune the XB properties of the chloroazaphosphatrane. Experiments are in progress in our laboratory in order to design anion receptors combining two or more chloroazaphosphatrane units or by associating them with other motifs for a more selective and efficient anion recognition.

EXPERIMENTAL SECTION

General Methods. All reactions were performed under an inert atmosphere of dry argon. ^{1}H, ^{13}C, ^{19}F, and ^{31}P NMR spectra were recorded on Bruker AC 300, Bruker AC 400, Bruker 500 HD, and Bruker Avance III 600 spectrometers. Chemical shifts are reported in ppm on the δ scale relative to residual $CHCl_3$ (δ_H = 7.26 ppm, δ_C = 77.16 ppm) and CH_3CN (δ_H = 1.94 ppm, δ_C = 1.32 and 118.26 ppm) as the internal references. High-resolution mass spectra (HRMS) were performed on a SYNAPT G2 HDMS (Waters) spectrometer equipped with an atmospheric pressure ionization source (API) that was pneumatically assisted. Infrared spectra were recorded on a Bruker TENSOR 27 Fourier Transform infrared spectrometer equipped with a single reflection diamond Attenuated Total Reflection accessory (Bruker A222). Anhydrous dichloromethane was obtained from the Solvent Purification System BRAUN MB-SPS800. Dry acetonitrile was purchased from chemical suppliers.

Synthesis of Chloroazaphosphatranes. Proazaphosphatranes (**1**) were first prepared according to a known procedure.[50,58,59,72] Under an atmosphere of argon, in a flame-dried Schlenk flask, azaphosphatrane **1-H$^+$·Cl$^-$** (1.0 equiv) was dissolved in dried CH_2Cl_2 (C = 0.16 mol·L^{-1}), *t*-BuOK (2.1 equiv) was added, and the reaction mixture was stirred at room temperature for 2 h. Then, the solvent was removed under vacuum, and anhydrous toluene (C = 0.075 mol·L^{-1}) was added. The reaction mixture was stirred for another 0.5 h, and then, the suspension was filtered under argon through a two-necked fritted glass funnel. Then, the solvent was removed under vacuum to give pure proazaphosphatrane **1**. The product was directly used for the following step.

To a flame-dried Schlenk tube was added freshly prepared proazaphosphatrane **1** (1.0 equiv), dried CH_2Cl_2 (C = 0.33 mol·L^{-1}), and hexachloroethane (1.02 equiv); the mixture was stirred under argon at room temperature for 2 h. The solvent was evaporated under vacuum, and the residual was washed three times by Et_2O to give the desired product **1-Cl$^+$·Cl$^-$**.

ClP(MeNCH$_2$CH$_2$)$_3$N][Cl] ***1a-Cl$^+$·Cl$^-$*** *(Known Compound).*[80] Beige solid; yield: 85% (562 mg); mp 65−66 °C. IR/cm^{-1}: 3565, 2960, 2727, 2517, 1647, 1465, 1229, 1142, 984, 884, 764, 723, 642. ^{1}H NMR ($CDCl_3$, 300 MHz) δ = 3.74 (td, J = 3.0 Hz, 6.0 Hz, 6H), 3.39 (dt, J = 6.0 Hz, 12.0 Hz, 6H), 2.95 (d, J = 15.0 Hz, 9H). ^{13}C NMR ($CDCl_3$, 75 MHz) δ = 46.4 (d, J = 9.7 Hz), 45.1 (d, J = 9.0 Hz), 39.8 (d, J = 6.0 Hz). ^{31}P NMR ($CDCl_3$, 120 MHz) δ = −26.02. HRMS (ESI): m/z [M]$^+$ calcd for $C_9H_{21}N_4ClP^+$ 251.1187; found: 251.1186.

ClP(iBuNCH$_2$CH$_2$)$_3$N][Cl] ***(1b-Cl$^+$·Cl$^-$)*** *(Known Compound).*[67] White solid; yield: 47% (206 mg); mp 125−127 °C. IR/cm^{-1}: 3379, 2958, 2827, 1668, 1651, 1466, 1388, 1282, 1111, 1077, 1057, 869, 774, 573. ^{1}H NMR ($CDCl_3$, 300 MHz) δ = 3.63 (td, J = 3.0 Hz, 6.0 Hz, 6H), 3.34 (dt, J = 6.0 Hz, 12.0 Hz, 6H), 3.12 (dd, J = 6.0 Hz, 15.0 Hz, 6H), 2.01 (sept, J = 6.0 Hz, 3H), 0.93 (d, J = 6.0 Hz, 3H). ^{13}C NMR ($CDCl_3$, 75 MHz) δ = 59.6 (d, J = 2.2 Hz), 46.1 (d, J = 9.0 Hz), 45.7 (d, J = 7.5 Hz), 28.5 (d, J = 4.5 Hz), 20.3. ^{31}P NMR ($CDCl_3$, 120 MHz) δ = −13.81. HRMS (ESI): m/z [M]$^+$ calcd for $C_{18}H_{39}N_4PCl^+$ 377.2595; found: 377.2593.

[ClP(BnNCH$_2$CH$_2$)$_3$N][Cl] ***(1c-Cl$^+$·Cl$^-$)***. White solid; yield: 86% (261 mg); mp 145 °C. IR/cm^{-1}: 3364, 3060, 2925, 2884, 1635, 1604, 1493, 1384, 1299, 1261, 1142, 1071, 1024, 971, 920, 865, 766, 696, 590, 510. ^{1}H NMR ($CDCl_3$, 300 MHz) δ = 7.40−7.24 (m, 15H), 4.68 (d, J = 14.7 Hz, 6H), 3.65 (td, J = 6.8, 4.3 Hz, 6H), 3.32 (dt, J = 12.0, 6.7 Hz, 6H). ^{13}C NMR ($CDCl_3$, 75 MHz) δ = 136.9 (d, J = 5.25 Hz), 129.1, 128.2, 127.7, 55.7 (d, J = 4.5 Hz), 44.5 (d, J = 9.75 Hz), 44.2 (d, J = 9.0 Hz). ^{31}P NMR ($CDCl_3$, 120 MHz) δ = −23.44. HRMS (ESI): m/z [M]$^+$ calcd for $C_{27}H_{33}ClN_4P^+$ 479.2126; found: 479.2126.

[ClP(p-OMe-BnNCH$_2$CH$_2$)$_3$N][Cl] ***(1d-Cl$^+$·Cl$^-$)*** *(Known Compound).*[81] White solid; yield: 46% (226 mg); mp 205 °C. IR/cm^{-1}: 3744, 3648, 3367, 2946, 2833, 2787, 2362, 1652, 1584, 1541, 1509, 1389, 1419, 1354, 1274, 1172, 1098, 945, 869, 816, 761, 657, 602, 572. ^{1}H NMR ($CDCl_3$, 300 MHz) δ = 7.21 (d, J = 8.7 Hz, 6H), 6.86 (d, J = 8.6 Hz, 6H), 4.59 (d, J = 14.7 Hz, 1H), 3.53 (td, J = 6.8, 4.5 Hz, 6H), 3.23 (dt, J = 13.0 Hz, 6.7 Hz, 6H). ^{13}C NMR ($CDCl_3$, 100 MHz) δ = 159.5, 129.3, 128.8 (d, J = 4.65 Hz), 114.3, 55.4, 54.9 (d, J = 4.14 Hz), 44.4 (d, J = 9.9 Hz), 43.9 (d, J = 9.59 Hz). ^{31}P NMR ($CDCl_3$, 120 MHz) δ = −23.38. HRMS (ESI): m/z [M]$^+$ calcd for $C_{30}H_{39}ClN_4O_3P^+$ 569.2443; found: 569.2441.

[ClP(p-CF$_3$-BnNCH$_2$CH$_2$)$_3$N][Cl] ***(1e-Cl$^+$·Cl$^-$)***. White solid; yield: 62% (196 mg); mp 155 °C. IR/cm^{-1}: 2327, 2245, 1996, 1781, 1698, 1635, 1622, 1576, 1507, 1473, 1418, 1395, 1157, 1066, 816, 764, 573. ^{1}H NMR ($CDCl_3$, 300 MHz) δ = 7.63 (d, J = 6.0 Hz, 6H), 7.41 (d, J = 9.0 Hz, 6H), 4.76 (d, J = 15.0 Hz, 6H), 3.91 (q, J = 6.0 Hz, 6H), 3.53 (dt, J = 6.0 Hz, 12.0 Hz, 6H). ^{13}C NMR (CD_3CN, 75 MHz) δ = 144.0 (dd, J = 1.5 Hz, 4.5 Hz), 129.6 (d, J = 31.5 Hz), 128.3, 126.4 (q, J = 3.75 Hz), 125.4 (d, J = 270 Hz), 55.5 (d, J = 5.25 Hz), 46.4 (d, J = 9.0 Hz), 45.5 (d, J = 9.0 Hz). ^{31}P NMR ($CDCl_3$, 120 MHz) δ = −23.82. ^{19}F NMR ($CDCl_3$, 376 MHz) δ = −62.60. HRMS (ESI): m/z [M]$^+$ calcd for $C_{30}H_{30}N_4F_9ClP^+$ 683.1747; found: 683.1747.

Anion Metathesis. In a flame-dried Schlenk flask were added dried acetonitrile (C = 0.1 mol·L^{-1}) and **1-Cl$^+$·Cl$^-$** (1.0 equiv). A solution of $NaPF_6$ (1.4 equiv) in dried acetonitrile (C = 0.26 mol·L^{-1}) was added dropwise, and the mixture was stirred for 2 h at room temperature. The solvent was evaporated under a vacuum, and dried acetone (C = 0.07 mol·L^{-1}) was added. White solid precipitate was observed. The supernatant was evaporated under a vacuum to give pure **1-Cl$^+$·PF$_6^-$**.

[ClP(MeNCH$_2$CH$_2$)$_3$N][PF$_6$] ***(1a-Cl$^+$·PF$_6^-$)***. Beige solid; yield: 70% (105 mg); mp 250 °C. IR/cm^{-1}: 2945, 1489, 1394, 1254, 1144, 973, 832, 746, 556. ^{1}H NMR (CD_3CN, 300 MHz) δ = 3.37−3.25 (m, 6H), 3.21−3.14 (m, 6H), 2.90 (d, J = 15.0 Hz, 9H). ^{13}C NMR (CD_3CN, 75 MHz) δ = 46.8 (d, J_{PC} = 9.0 Hz), 46.3 (d, J_{PC} = 9.7 Hz), 39.7 (d, J_{PC} = 6.0 Hz). ^{31}P NMR (CD_3CN, 120 MHz) δ = −21.34, −144.61 (sept, J_{P-F} = 697.2 Hz). ^{19}F NMR (CD_3CN, 376 MHz) δ = −71.64, −74.43. HRMS (ESI): m/z [M]$^+$ calcd for $C_9H_{21}N_4ClP^+$ 251.1187; found: 251.1187. X-ray: the product was crystallized from Et_2O/CH_3CN. CCDC 2060857 contains the supplementary crystallographic data for this paper.

[ClP(iBuNCH$_2$CH$_2$)$_3$N][PF$_6$] ***(1b-Cl$^+$·PF$_6^-$)***. White solid; yield: 65% (169 mg); mp 177 °C. IR/cm^{-1}: 2960, 2928, 2872, 1466, 1390, 1368, 1313, 1283, 1176, 1114, 1076, 1058, 833, 780, 595, 556. ^{1}H NMR ($CDCl_3$, 400 MHz) δ = 3.29 (dt, J = 4.0 Hz, 16.0 Hz, 6H), 3.16 (td, J = 4.0 Hz, 8.0 Hz, 6H), 3.09 (dd, J = 4.0 Hz, 12.0 Hz, 6H), 2.01 (sept, J = 8.0 Hz, 3H), 0.94 (d, J = 8.0 Hz, 3H). ^{13}C NMR ($CDCl_3$, 75 MHz) δ = 58.9 (d, J_{PC} = 1.5 Hz), 47.4 (d, J_{PC} = 9.7 Hz), 45.5 (d, J_{PC} = 6.7 Hz), 28.6 (d, J_{PC} = 5.2 Hz), 20.2. ^{31}P NMR ($CDCl_3$, 120 MHz) δ

= −4.32, −144.31 (sept, J_{PF} = 704.4 Hz). ^{19}F NMR ($CDCl_3$, 376 MHz) δ = −71.00, −73.52. HRMS (ESI): m/z $[M + H]^+$ calcd for $C_{18}H_{39}N_4PCl^+$ 377.2595; found: 377.2592.

*[ClP(BnNCH$_2$CH$_2$)$_3$N][PF$_6$] (**1c-Cl$^+$·PF$_6^-$**).* White solid; yield: 97% (252 mg); mp 137 °C. IR/cm^{-1}: 3648, 2892, 1604, 1494, 1454, 1396, 1303, 1201, 1145, 1106, 1049, 949, 833, 760, 697, 606, 592, 510. ^{1}H NMR (CD_3CN, 500 MHz) δ = 7.44−7.27 (m, 15H), 4.67 (d, J = 14.75 Hz, 6H), 3.35 (dt, J = 6.65 Hz, 12.85 Hz, 6H), 3.25 (td, J = 3.95 Hz, 6.4 Hz, 6H). ^{13}C NMR ($CDCl_3$, 75 MHz) δ = 136.9, 129.1, 128.1, 127.6, 55.5 (d, J_{PC} = 4.5 Hz), 45.1 (d, J_{PC} = 9.75 Hz), 44.1 (d, J_{PC} = 9.0 Hz). ^{31}P NMR ($CDCl_3$, 121 MHz) δ = −20.07, −144.28 (sept, J_{PF} = 710.65 Hz). ^{19}F NMR ($CDCl_3$, 376 MHz) δ = −70.56, −73.09. HRMS (ESI): m/z $[M]^+$ calcd for $C_{27}H_{33}ClN_4P^+$ 479.2126; found: 479.2131.

*[ClP(p-OMe-BnNCH$_2$CH$_2$)$_3$N][PF$_6$] (**1d-Cl$^+$·PF$_6^-$**).* Pale yellow solid; yield: 64% (119 mg); mp 260 °C. IR/cm^{-1}: 2935, 2838, 1610, 1585, 1510, 1457, 1354, 1282, 1207, 1175, 1097, 951, 903, 829, 739, 657, 555, 518. ^{1}H NMR ($CDCl_3$, 300 MHz) δ = 7.22 (d, J = 8.6 Hz, 6H), 6.86 (d, J = 8.7 Hz, 6H), 4.56 (d, J = 14.2 Hz, 6H), 3.22 (dt, J = 12.8, 6.4 Hz, 6H), 3.08 (td, J = 3.0 Hz, 6.0 Hz, 6H). ^{13}C NMR ($CDCl_3$, 75 MHz) δ = 159.6, 129.3, 128.7 (d, J = 5.2 Hz), 114.4, 55.5, 54.8 (d, J = 4.5 Hz), 45.0 (d, J = 9.7 Hz), 43.8 (d, J = 9.0 Hz). ^{31}P NMR ($CDCl_3$, 120 MHz) δ = −19.04, −144.30 (sept, J_{PF} = 704.4 Hz). ^{19}F NMR ($CDCl_3$, 376 MHz) δ = −70.42, −72.94. HRMS (ESI): m/z $[M]^+$ calcd for $C_{30}H_{39}ClN_4O_3P^+$ 569.2443; found: 569.2442.

*[ClP(p-CF$_3$-BnNCH$_2$CH$_2$)$_3$N][PF$_6$] (**1e-Cl$^+$·PF$_6^-$**).* White solid; yield: 87% (201 mg); mp 227 °C. IR/cm^{-1} 3566, 2027, 1697, 1472, 1288, 1065, 1016, 935, 869, 846, 831, 765, 719, 658, 557. ^{1}H NMR (CD_3CN, 300 MHz) δ = 7.70 (d, J = 9.0 Hz, 6H), 7.50 (d, J = 6.0 Hz, 6H), 4.72 (d, J = 15.0 Hz, 6H), 3.51−3.37 (m, 12H), 3.53 (dt, J = 6.0 Hz, 12.0 Hz, 6H). ^{13}C NMR (CD_3CN, 100 MHz) δ = 143.8 (d, J = 4.0 Hz), 129.7 (d, J = 32.0 Hz), 126.5 (q, J = 4.0 Hz), 125.4 (d, J = 269.0 Hz), 55.5 (d, J = 5.0 Hz), 46.3 (d, J = 10.0 Hz), 45.4 (d, J = 9.0 Hz). ^{31}P NMR (CD_3CN, 120 MHz) δ = −22.50, −144.63 (sept, J_{PF} = 698.4 Hz). ^{19}F NMR (CD_3CN, 376 MHz) δ = −62.65, −62.71, −62.98, −70.08, −72.01. HRMS (ESI): m/z $[M]^+$ calcd for $C_{30}H_{30}N_4F_9ClP^+$ 683.1747; found: 683.1747. X-ray: the product was crystallized from Et_2O/CH_3CN. CCDC 2060875 contains the supplementary crystallographic data for this paper.

NMR Titration Experiments. A solution of host **1-Cl$^+$·PF$_6^-$** (5.0 mM in CD_3CN, 500 μL) was titrated in NMR tubes with aliquots of a concentrated solution (50 mM in CD_3CN) of halide anions. The chemical shifts of the $N_{eq}CH_2$ protons of the host were measured after each addition and plotted as a function of the guest/host ratio ([G]/[H]). The association constant K_a was obtained by nonlinear least-squares fitting of these plots using the BINDFIT program.[73]

Experimental Procedure for TEPO Measurements. A stock solution of TEPO in CH_2Cl_2 with a concentration of 0.083 M was prepared in a glovebox. [ClP(*p*-CH$_3$O-BnNCH$_2$CH$_2$)$_3$N][BAr^F] (**1d-Cl$^+$·BAr^{F-}**, 0.0069 mmol, 1.6 equiv) was dissolved in 0.25 mL of CH_2Cl_2 and 0.2 mL of CD_2Cl_2 and transferred into the NMR tube. A 50 μL portion of TEPO stock solution (0.00415 mmol, 1.0 equiv) was added to the NMR tube. The ^{31}P NMR spectrum was recorded at room temperature, and the ^{31}P NMR chemical shift was compared to a standard TEPO solution to determine the $\Delta\delta(^{31}P)$ value (Figure S86).[79]

Determination of pK_a. To a solution of [P(*i*BuNCH$_2$CH$_2$)$_3$N] (**1b**, 23 mg, 0.070 mmol) in dry CD_3CN (0.50 mL) in an NMR tube was added about 0.019 mmol of [HP(BnNCH$_2$CH$_2$)$_3$N][Cl] (**1c-H$^+$·Cl$^-$**). The thermodynamic equilibrium was reached once the values of the integration of the ^{31}P NMR signals remained constant. The pK_a = −log K_a was then calculated (Figures S87 and S88).

Comparison of Chloroazaphosphatranes with Chloroimidazoliums. Proazaphosphatrane **1d** (50 mg, 0.094 mmol) was placed in a Schlenk tube and dissolved in dry CH_2Cl_2 (1.5 mL). A solution of chloroimidazolium **7** (37 mg, 0.098 mmol) in dry CH_2Cl_2 (1.5 mL) was then added dropwise. The mixture was stirred vigorously for 1 h at room temperature. Then, the solvent was removed with a vacuum pump to give a yellow solid. ^{31}P NMR was performed (120 MHz, $CDCl_3$): δ = −12.11, −22.05 ppm.

(1) Evans, N. H.; Beer, P. D. Advances in anion supramolecular chemistry: from recognition to chemical applications. *Angew. Chem., Int. Ed.* **2014**, *53*, 11716−11754.
(2) Sessler, J. L.; Gale, P. A.; Cho, W.-S. *Anion Receptor Chemistry*; Stoddart, J. F., Ed.; RSC Publishing: Cambridge, U.K., 2006.
(3) Gale, P. A.; Howe, E. N. W.; Wu, X. Anion receptor chemistry. *Chem.* **2016**, *1*, 351−422.
(4) Chen, L.; Berry, S. N.; Wu, X.; Howe, E. N. W.; Gale, P. A. Advances in anion receptor chemistry. *Chem.* **2020**, *6*, 61−141.
(5) Busschaert, N.; Caltagirone, C.; Van Rossom, W.; Gale, P. A. Applications of supramolecular anion recognition. *Chem. Rev.* **2015**, *115*, 8038−8155.
(6) Molina, P.; Zapata, F.; Caballero, A. Anion recognition strategies based on combined noncovalent interactions. *Chem. Rev.* **2017**, *117*, 9907−9972.
(7) Gale, P. A.; Howe, E. N. W.; Wu, X.; Spooner, M. J. Anion receptor chemistry: highlights from 2016. *Coord. Chem. Rev.* **2018**, *375*, 333−372.
(8) Gilday, L. C.; Robinson, S. W.; Barendt, T. A.; Langton, M. J.; Mullaney, B. R.; Beer, P. D. Halogen bonding in supramolecular chemistry. *Chem. Rev.* **2015**, *115*, 7118−7195.
(9) Ashton, T. D.; Jolliffe, K. A.; Pfeffer, F. M. Luminescent probes for the bioimaging of small anionic species in vitro and in vivo. *Chem. Soc. Rev.* **2015**, *44*, 4547−4595.
(10) Zhang, D.; Ronson, T. K.; Nitschke, J. R. Functional capsules via subcomponent self-assembly. *Acc. Chem. Res.* **2018**, *51*, 2423−2436.
(11) Kumar, R.; Sharma, A.; Singh, H.; Suating, P.; Kim, H. S.; Sunwoo, K.; Shim, I.; Gibb, B. C.; Kim, J. S. Revisiting fluorescent calixarenes: from molecular sensors to smart materials. *Chem. Rev.* **2019**, *119*, 9657−9721.
(12) Hein, R.; Beer, P. D.; Davis, J. J. Electrochemical anion sensing: supramolecular approaches. *Chem. Rev.* **2020**, *120*, 1888−1935.
(13) Li, H.; Valkenier, H.; Thorne, A. G.; Dias, C. M.; Cooper, J. A.; Kieffer, M.; Busschaert, N.; Gale, P. A.; Sheppard, D. N.; Davis, A. P. Anion carriers as potential treatments for cystic fibrosis: transport in cystic fibrosis cells, and additivity to channel-targeting drugs. *Chem. Sci.* **2019**, *10*, 9663−9672.
(14) Butler, S. J.; Jolliffe, K. A. Anion receptors for the discrimination of ATP and ADP in biological media. *ChemPlusChem* **2021**, *86*, 59−70.
(15) Butler, S. J.; Jolliffe, K. A. Molecular recognition and sensing of dicarboxylates and dicarboxylic acids. *Org. Biomol. Chem.* **2020**, *18*, 8236−8254.
(16) Zhao, Y.; Cotelle, Y.; Liu, L.; López-Andarias, J.; Bornhof, A.-B.; Akamatsu, M.; Sakai, N.; Matile, S. The emergence of anion−π catalysis. *Acc. Chem. Res.* **2018**, *51*, 2255−2263.
(17) Ballester, P. Experimental quantification of anion−π interactions in solution using neutral host−guest model systems. *Acc. Chem. Res.* **2013**, *46*, 874−884.
(18) Vargas Jentzsch, A.; Hennig, A.; Mareda, J.; Matile, S. Synthetic ion transporters that work with anion−π interactions, halogen bonds, and anion−macrodipole interactions. *Acc. Chem. Res.* **2013**, *46*, 2791−2800.
(19) Jones, J. S.; Gabbaï, F. P. Coordination- and redox-noninnocent behavior of ambiphilic ligands containing antimony. *Acc. Chem. Res.* **2016**, *49*, 857−867.
(20) Wade, C. R.; Broomsgrove, A. E. J.; Aldridge, S.; Gabbaï, F. P. Fluoride ion complexation and sensing using organoboron compounds. *Chem. Rev.* **2010**, *110*, 3958−3984.
(21) Jolliffe, K. A. Pyrophosphate recognition and sensing in water using bis[zinc(ii)dipicolylamino]-functionalized peptides. *Acc. Chem. Res.* **2017**, *50*, 2254−2263.
(22) Lim, J. Y. C.; Beer, P. D. Sigma-hole interactions in anion recognition. *Chem.* **2018**, *4*, 731−783.
(23) Taylor, M. S. Anion recognition based on halogen, chalcogen, pnictogen and tetrel bonding. *Coord. Chem. Rev.* **2020**, *413*, 213270.
(24) Vogel, L.; Wonner, P.; Huber, S. M. Chalcogen bonding: an overview. *Angew. Chem., Int. Ed.* **2019**, *58*, 1880−1891.
(25) Beau, M.; Lee, S.; Kim, S.; Han, W.-S.; Jeannin, O.; Fourmigué, M.; Aubert, E.; Espinosa, E.; Jeon, I.-R. Strong σ-hole activation on icosahedral carborane derivatives for a directional halide recognition. *Angew. Chem., Int. Ed.* **2021**, *60*, 366−370.
(26) Fourmigué, M.; Dhaka, A. Chalcogen bonding in crystalline diselenides and selenocyanates: From molecules of pharmaceutical interest to conducting materials. *Coord. Chem. Rev.* **2020**, *403*, 213084.
(27) Desiraju, G. R.; Ho, P. S.; Kloo, L.; Legon, A. C.; Marquardt, R.; Metrangolo, P.; Politzer, P.; Resnati, G.; Rissanen, K. Definition of the halogen bond. *Pure Appl. Chem.* **2013**, *85*, 1711−1713.
(28) Pancholi, J.; Beer, P. D. Halogen bonding motifs for anion recognition. *Coord. Chem. Rev.* **2020**, *416*, 213281.
(29) Metrangolo, P.; Resnati, G.; Pilati, T.; Biella, S. Halogen bonding in crystal engineering. *Struct. Bonding (Berlin)* **2008**, *126*, 105−136.
(30) Fourmigué, M. Halogen bonding in conducting or magnetic molecular materials. *Struct. Bonding (Berlin)* **2008**, *126*, 181−207.
(31) Hachem, H.; Jeannin, O.; Fourmigué, M.; Barrière, F.; Lorcy, D. Halogen bonded metal bis(dithiolene) 2D frameworks. *CrystEngComm* **2020**, *22*, 3579−3587.
(32) Cavallo, G.; Metrangolo, P.; Milani, R.; Pilati, T.; Priimagi, A.; Resnati, G.; Terraneo, G. The halogen bond. *Chem. Rev.* **2016**, *116*, 2478−2601.
(33) Tepper, R.; Schubert, U. S. Halogen bonding in solution: anion recognition, templated self-assembly, and organocatalysis. *Angew. Chem., Int. Ed.* **2018**, *57*, 6004−6016.
(34) Bulfield, D.; Huber, S. M. Halogen bonding in organic synthesis and organocatalysis. *Chem. - Eur. J.* **2016**, *22*, 14434−14450.
(35) Jentzsch, A. V.; Matile, S. Anion transport with halogen bonds. *Top. Curr. Chem.* **2014**, *358*, 205−239.
(36) Hijazi, H.; Vacher, A.; Groni, S.; Lorcy, D.; Levillain, E.; Fave, C.; Schöllhorn, B. Electrochemically driven interfacial halogen bonding on self-assembled monolayers for anion detection. *Chem. Commun.* **2019**, *55*, 1983−1986.
(37) Fave, C.; Schöllhorn, B. Electrochemical activation of halogen bonding. *Current Opinion in Electrochemistry* **2019**, *15*, 89−96.
(38) Pizzi, A.; Pigliacelli, C.; Bergamaschi, G.; Gori, A.; Metrangolo, P. Biomimetic engineering of the molecular recognition and self-assembly of peptides and proteins *via* halogenation. *Coord. Chem. Rev.* **2020**, *411*, 213242.
(39) Bergamaschi, G.; Lascialfari, L.; Pizzi, A.; Martinez Espinoza, M. I.; Demitri, N.; Milani, A.; Gori, A.; Metrangolo, P. A halogen bond-donor amino acid for organocatalysis in water. *Chem. Commun.* **2018**, *54*, 10718−10721.
(40) Bamberger, J.; Ostler, F.; García Mancheño, O. Frontiers in halogen and chalcogen-bond donor organocatalysis. *ChemCatChem* **2019**, *11*, 5198−5211.
(41) Ostler, F.; Piekarski, D. G.; Danelzik, T.; Taylor, M. S.; García Mancheño, O. Neutral chiral tetrakis-iodo-triazole halogen-bond donor for chiral recognition and enantioselective catalysis. *Chem. - Eur. J.* **2021**, *27*, 2315−2320.
(42) Caballero, A.; Zapata, F.; Beer, P. D. Interlocked host molecules for anion recognition and sensing. *Coord. Chem. Rev.* **2013**, *257*, 2434−2455.

(43) Klein, H. A.; Kuhna, H.; Beer, P. D. Anion and pH dependent molecular motion by a halogen bonding [2]rotaxane. *Chem. Commun.* **2019**, *55*, 9975−9978.
(44) Bunchuay, T.; Docker, A.; Martinez-Martinez, A. J.; Beer, P. D. A potent halogen-bonding donor motif for anion recognition and anion template mechanical bond synthesis. *Angew. Chem., Int. Ed.* **2019**, *58*, 13823−13827.
(45) Borissov, A.; Marques, I.; Lim, J. Y. C.; Félix, V.; Smith, M. D.; Beer, P. D. Anion recognition in water by charge-neutral halogen and chalcogen bonding foldamer receptors. *J. Am. Chem. Soc.* **2019**, *141*, 4119−4129.
(46) Klein, H. A.; Beer, P. D. Iodide discrimination by tetraiodotriazole halogen bonding interlocked hosts. *Chem. - Eur. J.* **2019**, *25*, 3125−3130.
(47) Li, X.; Lim, J. Y. C.; Beer, P. D. Acid-regulated switching of metal cation and anion guest binding in halogen-bonding rotaxanes. *Chem. - Eur. J.* **2018**, *24*, 17788−17795.
(48) Verkade, J. G. Main group atranes: chemical and structural features. *Coord. Chem. Rev.* **1994**, *137*, 233−295.
(49) Lensink, C.; Xi, S.-K.; Daniels, L. M.; Verkade, J. G. The unusually robust phosphorus-hydrogen bond in the novel cation [cyclic] $HP(NMeCH_2CH_2)_3N^+$. *J. Am. Chem. Soc.* **1989**, *111*, 3478−3479.
(50) Laramay, M. A.; Verkade, J. G. The "anomalous" basicity of $P(NHCH_2CH_2)_3N$ relative to $P(NMeCH_2CH_2)_3N$ and $P(NBzCH_2CH_2)_3N$: a chemical consequence of orbital charge balance? *J. Am. Chem. Soc.* **1990**, *112*, 9421−9422.
(51) Verkade, J. G.; Kisanga, P. B. Proazaphosphatranes: a synthesis methodology trip from their discovery to vitamin A. *Tetrahedron* **2003**, *59*, 7819−7858.
(52) Thammavongsy, Z.; Khosrowabadi Kotyk, J. F.; Tsay, C.; Yang, J. Y. Flexibility is key: synthesis of a tripyridylamine (TPA) congener with a phosphorus apical donor and coordination to cobalt(II). *Inorg. Chem.* **2015**, *54*, 11505−11510.
(53) Thammavongsy, Z.; Kha, I. M.; Ziller, J. W.; Yang, J. Y. Electronic and steric Tolman parameters for proazaphosphatranes, the superbase core of the tri(pyridylmethyl)azaphosphatrane (TPAP) ligand. *Dalton Trans.* **2016**, *45*, 9853−9859.
(54) Sutthirat, N.; Ziller, J. W.; Yang, J. Y.; Thammavongsy, Z. Crystal structure of $NiFe(CO)_5$[tris(pyridylmethyl)-azaphosphatrane]: a synthetic mimic of the NiFe hydrogenase active site incorporating a pendant pyridine base. *Acta Crystallogr.* **2019**, *E75*, 438−442.
(55) Thammavongsy, Z.; Cunningham, D. W.; Sutthirat, N.; Eisenhart, R. J.; Ziller, J. W.; Yang, J. Y. Adaptable ligand donor strength: tracking transannular bond interactions in tris(2-pyridylmethyl)-azaphosphatrane (TPAP). *Dalton Trans.* **2018**, *47*, 14101−14110.
(56) Chatelet, B.; Nava, P.; Clavier, H.; Martinez, A. Synthesis of gold(I) complexes bearing Verkade's superbases. *Eur. J. Inorg. Chem.* **2017**, *2017*, 4311−4316.
(57) Yang, J.; Chatelet, B.; Ziarelli, F.; Dufaud, V.; Hérault, D.; Martinez, A. Verkade's superbase as an organocatalyst for the Strecker reaction. *Eur. J. Org. Chem.* **2018**, *2018*, 6328−6332.
(58) Raytchev, P. D.; Martinez, A.; Gornitzka, H.; Dutasta, J.-P. Encaging the Verkade's superbases: thermodynamic and kinetic consequences. *J. Am. Chem. Soc.* **2011**, *133*, 2157−2159.
(59) Chatelet, B.; Gornitzka, H.; Dufaud, V.; Jeanneau, E.; Dutasta, J.-P.; Martinez, A. Superbases in confined space: control of the basicity and reactivity of the proton transfer. *J. Am. Chem. Soc.* **2013**, *135*, 18659−18664.
(60) Kisanga, P. B.; Verkade, J. G.; Schwesinger, R. pK_a Measurements of $P(RNCH_2CH_3)_3N$. *J. Org. Chem.* **2000**, *65*, 5431−5432.
(61) Zhang, D.; Ronson, T. K.; Mosquera, J.; Martinez, A.; Nitschke, J. R. Selective anion extraction and recovery using a $Fe^{II}_4L_4$ cage. *Angew. Chem., Int. Ed.* **2018**, *57*, 3717−3721.
(62) Zhang, D.; Ronson, T. K.; Mosquera, J.; Martinez, A.; Guy, L.; Nitschke, J. R. Anion binding in water drives structural adaptation in an azaphosphatrane-functionalized $Fe^{II}_4L_4$ tetrahedron. *J. Am. Chem. Soc.* **2017**, *139*, 6574−6577.
(63) Zhang, D.; Jardel, D.; Peruch, F.; Calin, N.; Dufaud, V.; Dutasta, J.-P.; Martinez, A.; Bibal, B. Azaphosphatranes as hydrogen-bonding organocatalysts for the activation of carbonyl group: investigation of lactide ring-opening polymerization. *Eur. J. Org. Chem.* **2016**, *2016*, 1619−1624.
(64) Chatelet, B.; Joucla, L.; Dutasta, J.-P.; Martinez, A.; Szeto, K. C.; Dufaud, V. Azaphosphatranes as structurally tunable organocatalysts for carbonate synthesis from CO_2 and epoxides. *J. Am. Chem. Soc.* **2013**, *135*, 5348−5351.
(65) Yang, J.; Manick, A.-D.; Li, C.; Bugaut, X.; Chatelet, B.; Dufaud, V.; Hérault, D.; Martinez, A. Azaphosphatranes catalyzed Strecker reaction in the presence of water. *ChemistrySelect* **2020**, *5*, 14764−14767.
(66) Liu, X.-D.; Verkade, J. G. Unusual phosphoryl donor properties of O = $P(MeNCH_2CH_2)_3N$. *Inorg. Chem.* **1998**, *37*, 5189−5197.
(67) Matthews, A. D.; Prasad, S.; Schley, N. D.; Donald, K. J.; Johnson, M. W. On transannulation in azaphosphatranes: synthesis and theoretical analysis. *Inorg. Chem.* **2019**, *58*, 15983−15992.
(68) Johnstone, T. C.; Briceno-Strocchia, A. I.; Stephan, D. W. Frustrated Lewis pair oxidation permits synthesis of a fluoroazaphosphatrane, [FP(MeNCH2CH2)3N]+. *Inorg. Chem.* **2018**, *57*, 15299−15304.
(69) Sarwar, M. G.; Dragisić, B.; Dimitrijević, E.; Taylor, M. S. Halogen bonding between anions and iodoperfluoroorganics: solution-phase thermodynamics and multidentate-receptor design. *Chem. - Eur. J.* **2013**, *19*, 2050−2058.
(70) Cametti, M.; Raatikainen, K.; Metrangolo, P.; Pilati, T.; Terraneoa, G.; Resnati, G. 2-Iodo-imidazolium receptor binds oxoanions via charge-assisted halogen bonding. *Org. Biomol. Chem.* **2012**, *10*, 1329−1333.
(71) Chintareddy, V. R.; Wadhwa, K.; Verkade, J. G. P-$(PhCH_2NCH_2CH_2)_3N$ Catalysis of Mukaiyama aldol reactions of aliphatic, aromatic, and heterocyclic aldehydes and trifluoromethyl phenyl ketone. *J. Org. Chem.* **2009**, *74*, 8118−8132.
(72) Kisanga, P. B.; Verkade, J. G. Synthesis of new proazaphosphatranes and their application in organic synthesis. *Tetrahedron* **2001**, *57*, 467−475.
(73) Brynn Hibbert, D.; Thordarson, P. The death of the Job plot, transparency, open science and online tools, uncertainty estimation methods and other developments in supramolecular chemistry data analysis. *Chem. Commun.* **2016**, *52*, 12792−12805.
(74) Thordarson, P. Determining association constants from titration experiments in supramolecular chemistry. *Chem. Soc. Rev.* **2011**, *40*, 1305−1323.
(75) Laurence, C.; Graton, J.; Berthelot, M.; El Ghomari, M. J. The diiodine basicity scale: toward a general halogen-bond basicity scale. *Chem. - Eur. J.* **2011**, *17*, 10431−10444.
(76) Ostras', A. S.; Ivanov, D. M.; Novikov, A. S.; Tolstoy, P. M. Phosphine oxides as spectroscopic halogen bond descriptors: IR and NMR correlations with interatomic distances and complexation energy. *Molecules* **2020**, *25*, 1406−1423.
(77) Mayer, U.; Gutmann, V.; Gerger, W. The acceptor number − a quantitative empirical parameter for the electrophilic properties of solvents. *Monatsh. Chem.* **1975**, *106*, 1235−1257.
(78) Beckett, M. A.; Strickland, G. C.; Holland, J. R.; Varma, K. S. A convenient NMR method for the measurement of Lewis acidity at boron centres: correlation of reaction rates of Lewis acid initiated epoxide polymerizations with Lewis acidity. *Polymer* **1996**, *37*, 4629−4631.
(79) Chang, Y.-P.; Tang, T.; Jagannathan, J. R.; Hirbawi, N.; Sun, S.; Brown, J.; Franz, A. K. NMR quantification of halogen-bonding ability to evaluate catalyst activity. *Org. Lett.* **2020**, *22*, 6647−6652.
(80) Gudat, D.; Lensink, C.; Schmidt, H.; Xi, S.-K.; Verkade, J. G. Novel properties of new azaphosphatranes and silatranes. *Phosphorus, Sulfur Silicon Relat. Elem.* **1989**, *41*, 21−29.
(81) Yang, J.; Chatelet, B.; Dufaud, V.; Hérault, D.; Michaud-Chevalier, S.; Robert, V.; Dutasta, J.-P.; Martinez, A. Endohedral

functionalized cage as a tool to create frustrated Lewis pairs. *Angew. Chem.* **2018**, *130*, 14408−14411.
(82) Bruckmann, H. A.; Pena, M. A.; Bolm, C. Organocatalysis through Halogen-Bond Activation. *Synlett* **2008**, *2008*, 900−902.
(83) (a) Haraguchi, R.; Hoshino, S.; Sakai, M.; Tanazawa, S.; Morita, Y.; Komatsu, T.; Fukuzawa, S. Bulky iodotriazolium tetrafluoroborates as highly active halogen-bonding-donor catalysts. *Chem. Commun.* **2018**, *54*, 10320−10323. (b) Kaasik, M.; Metsala, A.; Kaabel, S.; Kriis, K.; Järving, I.; Kanger, T. Halo-1,2,3-triazolium Salts as Halogen Bond Donors for the Activation of Imines in Dihydropyridinone Synthesis. *J. Org. Chem.* **2019**, *84*, 4294−4303. (c) Jungbauer, S. H.; Walter, S. M.; Schindler, S.; Rout, L.; Kniep, F.; Huber, S. M. Activation of a carbonyl compound by halogen bonding. *Chem. Commun.* **2014**, *50*, 6281−6284. (d) Takeda, Y.; Hisakuni, D.; Lin, C.-H.; Minakata, S. 2-Halogenoimidazolium Salt Catalyzed Aza-Diels−Alder Reaction through Halogen-Bond Formation. *Org. Lett.* **2015**, *17*, 318−321.
(84) (a) Benz, S.; Poblador-Bahamonde, A. I.; Low-Ders, N.; Matile, S. Catalysis with Pnictogen, Chalcogen, and Halogen Bonds. *Angew. Chem., Int. Ed.* **2018**, *57*, 5408−5412. (b) Jungbauer, S. H.; Huber, S. M. Cationic Multidentate Halogen-Bond Donors in Halide Abstraction Organocatalysis: Catalyst Optimization by Preorganization. *J. Am. Chem. Soc.* **2015**, *137*, 12110−12120. (c) Dreger, A.; Engelage, E.; Mallick, B.; Beer, P. D.; Huber, S. M. The role of charge in 1,2,3-triazol(ium)-based halogen bonding activators. *Chem. Commun.* **2018**, *54*, 4013−4016. (d) Kniep, F.; Walter, S. M.; Herdtweck, E.; Huber, S. M. 4,4′-Azobis(halopyridinium) Derivatives: Strong Multidentate Halogen-Bond Donors with a Redox-Active Core. *Chem. - Eur. J.* **2012**, *18*, 1306−1310. (e) Walter, S. M.; Kniep, F.; Herdtweck, E.; Huber, S. M. Halogen-Bond-Induced Activation of a Carbon−Heteroatom Bond. *Angew. Chem., Int. Ed.* **2011**, *50*, 7187−7191. (f) Kniep, F.; Rout, L.; Walter, S. M.; Bensch, H. K. V.; Jungbauer, S. H.; Herdtweck, E.; Huber, S. M. 5- Iodo-1,2,3-triazolium-based multidentate halogen-bond donors as activating reagents. *Chem. Commun.* **2012**, *48*, 9299−9301.
(85) (a) Gliese, J.-P.; Jungbauer, S. H.; Huber, S. M. A halogen-bonding-catalyzed Michael addition reaction. *Chem. Commun.* **2017**, *53*, 12052−12055. (b) von der Heiden, D.; Detmar, E.; Kuchta, R.; Breugst, M. Activation of Michael Acceptors by Halogen-Bond Donors. *Synlett* **2018**, *29*, 1307−1313.